


Review

Catestatin: Antimicrobial Functions and Potential Therapeutics

Suborno Jati ^{1,†}, Sumana Mahata ^{2,†}, Soumita Das ³, Saurabh Chatterjee ⁴  and Sushil K. Mahata ^{2,5,*,‡}

¹ Department of Chemistry and Biochemistry, University of California San Diego, La Jolla, CA 92093, USA; sjati@ucsd.edu

² Department of Medicine, University of California San Diego, La Jolla, CA 92093, USA; sumahata@health.ucsd.edu

³ Department of Biomedical and Nutritional Science, University of Massachusetts Lowell, Lowell, MA 01854, USA; soumita_das@uml.edu

⁴ Department of Medicine, University of California Irvine, Irvine, CA 92697, USA; saurabh@hs.uci.edu

⁵ VA San Diego Healthcare System, 3350 La Jolla Village Drive, San Diego, CA 92161, USA

* Correspondence: smahata@health.ucsd.edu; Tel.: +1-(858)-552-8585 (ext. 2637)

† These authors contributed equally to this work.

‡ Dedicated to Marie Helene Metz-Boutigue for establishing catestatin as an antimicrobial and a cell permeable peptide.

Abstract: The rapid increase in drug-resistant and multidrug-resistant infections poses a serious challenge to antimicrobial therapies, and has created a global health crisis. Since antimicrobial peptides (AMPs) have escaped bacterial resistance throughout evolution, AMPs are a category of potential alternatives for antibiotic-resistant “superbugs”. The Chromogranin A (CgA)-derived peptide Catestatin (CST: hCgA_{352–372}; bCgA_{344–364}) was initially identified in 1997 as an acute nicotinic-cholinergic antagonist. Subsequently, CST was established as a pleiotropic hormone. In 2005, it was reported that N-terminal 15 amino acids of bovine CST (bCST_{1–15} aka cateslytin) exert antibacterial, antifungal, and antiyeast effects without showing any hemolytic effects. In 2017, D-bCST_{1–15} (where L-amino acids were changed to D-amino acids) was shown to exert very effective antimicrobial effects against various bacterial strains. Beyond antimicrobial effects, D-bCST_{1–15} potentiated (additive/synergistic) antibacterial effects of cefotaxime, amoxicillin, and methicillin. Furthermore, D-bCST_{1–15} neither triggered bacterial resistance nor elicited cytokine release. The present review will highlight the antimicrobial effects of CST, bCST_{1–15} (aka cateslytin), D-bCST_{1–15}, and human variants of CST (Gly364Ser-CST and Pro370Leu-CST); evolutionary conservation of CST in mammals; and their potential as a therapy for antibiotic-resistant “superbugs”.

Keywords: Chromogranin A; catestatin; gut microbiome; antimicrobial peptide; cell permeable peptide



Citation: Jati, S.; Mahata, S.; Das, S.; Chatterjee, S.; Mahata, S.K.

Catestatin: Antimicrobial Functions and Potential Therapeutics.

Pharmaceutics **2023**, *15*, 1550.

[https://doi.org/10.3390/](https://doi.org/10.3390/pharmaceutics15051550)

[pharmaceutics15051550](https://doi.org/10.3390/pharmaceutics15051550)

Academic Editors: Scavello

Francesco, Jean-Eric Ghia and

Amiche Mohamed

Received: 1 April 2023

Revised: 9 May 2023

Accepted: 14 May 2023

Published: 20 May 2023



Copyright: © 2023 by the authors. Licensee MDPI, Basel, Switzerland. This article is an open access article distributed under the terms and conditions of the Creative Commons Attribution (CC BY) license (<https://creativecommons.org/licenses/by/4.0/>).

1. Introduction

Microbial infections in critically ill patients are a global threat. With failing host defense, the use of antibiotics has taken the place for containment of those infections. Nevertheless, the microbes have also evolved with time to develop resistance against those drugs. This arm’s race between antibiotic drugs and pathogens had led to the rise of multi-drug-resistant microbes, called “superbugs”, which emphasizes the urgent need to develop new modes of treatment. Since antimicrobial peptides (AMPs) have evaded bacterial resistance for millions of years of evolution [1], AMPs could be a potential solution for antibiotic resistant “superbugs”. Chromogranin A (CgA), the acidic and secretory pro-protein [2,3], is proteolytically cleaved to generate several biologically important peptides, including Catestatin (CST: hCgA_{352–372}) [4–12]. The 21 amino acid peptide CST (human: S₃₅₂SMKLSFRARAYGFRGPGPQL₃₇₂; bovine: R₃₄₄SMRLSFRARGYGFRGPGPQL₃₆₄) was identified in 1997 as a physiological brake in catecholamine secretion, which acts by non-competitive inhibition of nicotinic-cholinergic signaling [5,13–18]. CST is now established as a pleiotropic peptide [6,19,20]

The non-hemolytic antimicrobial (bacteria, fungus, and yeast) effects of CST (bcCST_{1–15} aka cateslytin) were first reported in 2005, where CST was shown to act by penetrating fungal and yeast cell membranes [21]. The study showed that less than 10 µM peptide was required to kill the bacteria. Antibacterial activities were also reported for the two human variants of CST (G₃₆₄S-CST and P₃₇₀L-CST) [22] with minimal inhibitory concentration (MIC) of 1–20 µM [21]. Later, D-bCST_{1–15} (where L-amino acids were changed to D-amino acids: r₃₄₄smrlsfrargygr₃₅₈) was shown to exert more potent antibacterial (both Gram-positive and Gram-negative bacteria) effects than natural CST [23]. The present review will focus on the antimicrobial effects of CST, with special emphasis on the mechanisms underlying its antibacterial effects, therapeutic potential, and evolutionary conservation.

2. Antibacterial Effects of CST

2.1. Inhibition of Bacterial Growth by CST

The group of Metz-Boutigue first demonstrated the antibacterial activity of CST. Her group used bcCST_{344–358} (coining the term cateslytin to describe this antimicrobial effect) to reveal the inhibition of growth of the Gram-positive and Gram-negative bacteria [21]. The minimal inhibitory concentrations (MICs) of CST (bcCgA_{344–358}, hCgA_{352–372}, Gly₃₆₄Ser-CST and Pro₃₇₀Leu-CST) for Gram-positive bacteria (*Micrococcus luteus*, *Bacillus megaterium*, Group A *Streptococcus*, *S. aureus* ATCC 25923, *S. aureus* ATCC 49775, *S. aureus* S1 MRSA, *S. aureus* S1 MSSA, and *S. aureus* DmprF) range from 0.8 µM to >100 µM (Figure 1) [21,24]. The minimal concentration with 100% inhibition (MIC₁₀₀) for Gram-positive bacteria range from 2 µM to >100 µM. The MIC of CST was higher (8 µM to 50 µM) for Gram-negative bacteria (*Escherichia coli* D22, *E. coli* O29, and *Pseudomonas aeruginosa*) compared to Gram-positive bacteria (Figure 1). Likewise, the MIC₁₀₀ of CST was higher (15 µM to 150 µM) for Gram-negative bacteria compared to Gram-positive bacteria (Figure 1). The higher MIC and MIC₁₀₀ values of CST for Gram-negative bacteria are consistent with the presence of extra outer membrane containing lipopolysaccharide (LPS) [25,26]. Beyond the extra-thick cell membrane, Gram-negative bacteria also release exotoxins such as tetanus [27] and cholera toxins [28] that worsen prognosis.

Bacterial species	WT-CST bcCgA _{344–358} MIC (µM)	WT-CST bcCgA _{344–358} MIC ₁₀₀ (µM)	WT-CST hCgA _{352–372} MIC (µM)	WT-CST hCgA _{352–372} MIC ₁₀₀ (µM)	G364S-CST hCgA _{352–372} MIC (µM)	G364S-CST hCgA _{352–372} MIC ₁₀₀ (µM)	P370L-CST hCgA _{352–372} MIC (µM)	P370L-CST hCgA _{352–372} MIC ₁₀₀ (µM)
Gram-positive bacteria								
<i>Micrococcus luteus</i>	0.8	2	5	15	1	2	2	10
<i>Bacillus megaterium</i>	0.8	2	-	-	-	-	-	-
Group A <i>Streptococcus</i>			75	75		30		30-50
<i>Staphylococcus aureus</i> ATCC 25923	40		>100	>100	>100	>100		
<i>Staphylococcus aureus</i> ATCC 49775	37		125					
<i>Staphylococcus aureus</i> S1 (MRSA)	37		130					
<i>Staphylococcus aureus</i> S1 (MSSA)	45		150					
<i>Staphylococcus aureus</i> ΔmprF			20	30	5-10	10	5	5
Gram-negative bacteria								
<i>Escherichia coli</i> D22	8	15	15	150	10	40	20	100
<i>Escherichia coli</i> O29			30	30	20	20-30	10	5-10
<i>Pseudomonas aeruginosa</i>			50	50				

Figure 1. Effects of wild-type (WT)-CST and natural human variants of CST (Gly364Ser and Pro370Leu) on the growth of Gram-positive and Gram-negative bacteria showing minimal inhibitory concentration (MIC) and lethal concentration (MIC₁₀₀) of CST.

D-bCST_{1–15} was reported to exert more effective antimicrobial effects against various bacterial strains than L-bCST_{1–15} [23]. In addition to its antimicrobial effects, D-bCST_{1–15} was reported to potentiate (additive/synergistic) the antibacterial effects of cefotaxime,

amoxicillin, and methicillin [23]. Furthermore, it has been shown that D-bCST_{1–15} neither triggered bacterial resistance nor elicited cytokine release [23]. In addition, D-bCST_{1–15} was reported to be more resistant to degradation by secreted bacterial protease than L-bCST_{1–15} [23]. Thus, it was suggested that D-bCST_{1–15} can be used as a monotherapy or as a combination therapy with currently prescribed antibiotics to counteract various diseases associated with bacterial infection [23].

2.2. Composition of Bacterial Membranes

While antibiotics target specific cellular activities (e.g., synthesis of DNA, protein, or cell wall), AMPs target the LPS layer of the cell membrane. Extensive studies have been conducted to learn the composition of the bacterial membrane. The bacterial cytoplasmic membrane consists of zwitterionic phospholipids (phosphatidylcholine, phosphatidylethanolamine, sphingomyelin, etc.) and anionic phospholipids (phosphatidyl serine, phosphatidyl glycerol, etc.), providing them with a negative charge [29–32]. In contrast, besides the cytoplasmic membrane, Gram-negative bacteria contain an additional strong electronegative LPS-containing thick outer membrane [25,26]. Furthermore, the peptidoglycan layer on the outer side of the cytoplasmic membrane is much thicker in Gram-positive bacteria compared to Gram-negative bacteria (20–80 nm versus ~10 nm) [33,34]. The peptidoglycan layer in Gram-positive bacteria is connected by electronegative wall lipoteichoic acids and anchored on the phospholipid bilayer by electronegative lipoteichoic acids [35]. In contrast, in Gram-negative bacteria, the LPS forms the major lipid component of the outer leaflet of the outer membrane [35].

2.3. Secondary Structure of CST Explains the Antibacterial Effects of CST

Based on their secondary structure, AMPs are generally categorized into four groups: (i) α -helical AMPs, (ii) β -sheet AMPs, (iii) extended AMPs, and cationic loop AMPs [36]. Homology modeling followed by molecular dynamics simulation of bovine CST (bCgA_{342–370}) performed in a water shell led to a β -strand-loop- β -strand structure. Molecular dynamics and computer simulations of human CST_{1–21} revealed the following: R₁₀, A₁₁, and Y₁₂ contribute to a 3_{10} helix [37]. In contrast, F₇, R₈, A₉, F₁₄, R₁₅, G₁₆, P₁₇, and G₁₈ contribute to the antiparallel β -sheet [37]. The mechanism of the antibacterial action of CST_{1–21} could start by interacting with negatively charged moieties such as LPS in the outer membranes of Gram-negative bacteria and lipoteichoic acid in the wall of Gram-positive bacteria. The primary structure of CST reveals that CST contains cationic and hydrophobic residues and adopt a β -sheet secondary structure via intermolecular forces [38]. This folding structure would facilitate CST to fold into an amphiphilic conformation with positively charged (polar) and hydrophobic (nonpolar) faces (Figure 2). The presence of a great number of positively charged residues (5 in bCST and 4 in hCST) will allow CST to interact preferentially with negatively charged bacterial membranes [1,39]. Since the hydrophilic and hydrophobic amino acids of CST are structurally segregated, it will provide solubility of CST in both aqueous and lipid-rich environments, as suggested for other AMPs [40]. In addition, positively charged amino acids in CST formed amphipathic structures, as evidenced by separated hydrophobic and hydrophilic surface domains [39,41] (Figure 2). When the concentration of CST would exceed a certain critical concentration, the cell membrane would form pores, leading to content leakage, cell lysis, and finally death. Since cyclization of peptide has been reported to induce high antimicrobial activity [39,41], it is reasonable to assume that cyclization of CST would markedly improve the antibacterial activity of CST.

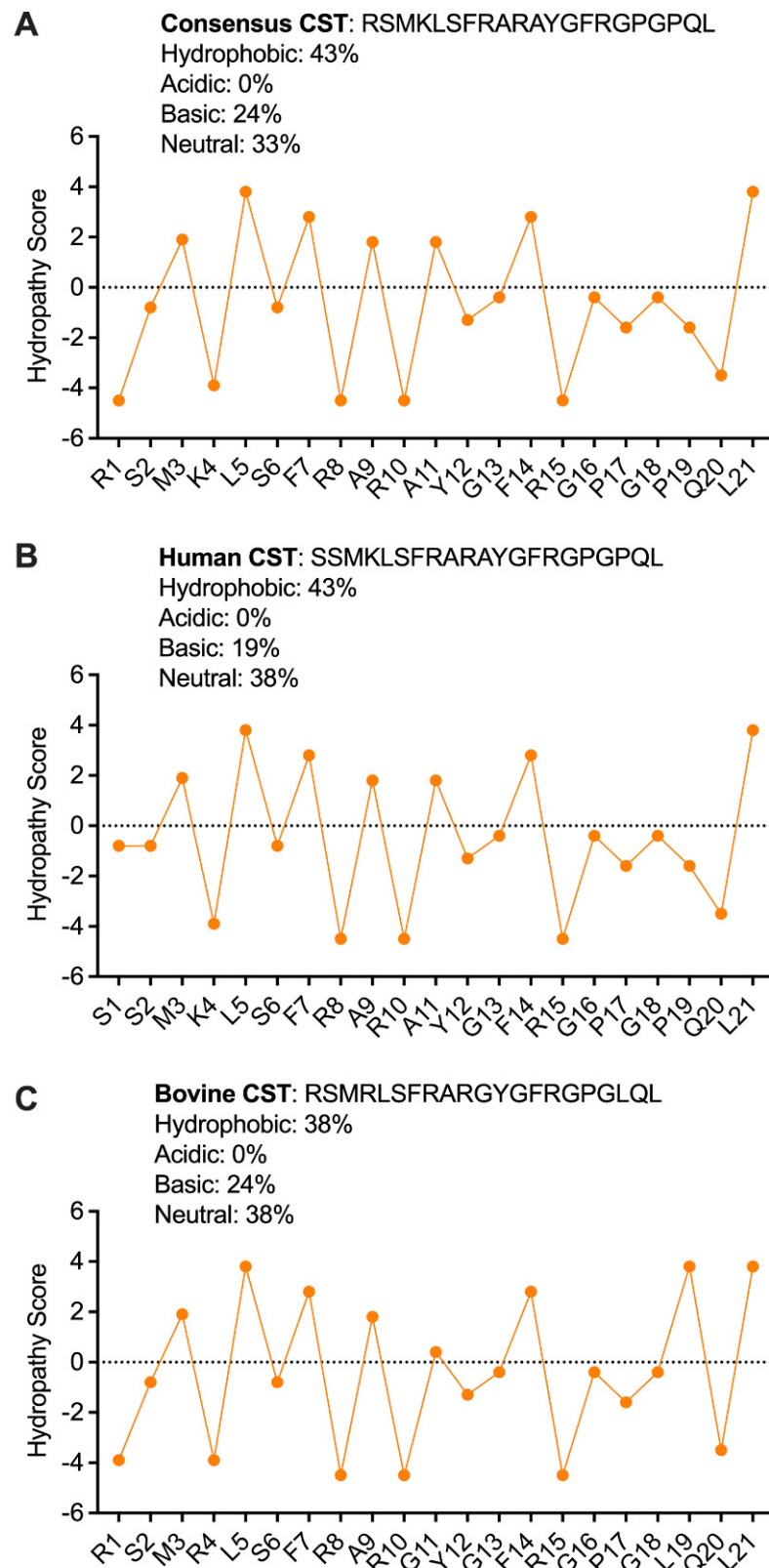


Figure 2. Hydropathy profiles of (A) Consensus CST, (B) Human CST, and (C) Bovine CST. The values are plotted based on the parameters used from Kyte and Doolittle, 1982. The values above zero represents the hydrophobic property of the amino acids that might contribute to the hydrophobic core of the peptide. The values below zero represent the hydrophilic property of the amino acids, which are instrumental in interaction with other protein factors.

Metz-Boutigue's group has shown that bCgA_{344–358} is unstructured in solution but is converted to an antiparallel β -structure and forms aggregates at the surface of negatively charged bacterial membranes [42]. As for catecholamine secretion [15], arginine residues were found to be crucial for binding to negatively charged lipids [42,43]. They proposed that the phase boundary defects caused by zones of different rigidity and thickness lead to permeability induction and peptide crossing through the bacterial membrane [42]. The fact that CST penetrates through the bacterial wall was shown by measuring the optical density of the released β -galactosidase from ML-35p [24]. Electron microscopical studies of *E. coli* ML-35p confirmed that CST rapidly disrupts the *E. coli* membrane, with visible membrane blebbing compared to untreated cells within 10 min [24].

2.4. CST as a Potential Therapy for Bacterial Diseases

AMPs derived from CgA display antimicrobial activities by lytic effects at micromolar range against Gram-positive bacteria, filamentous fungi, and yeasts. Interestingly, CST-derived peptides can kill “superbugs” and more particularly *S. aureus* [44]. Considering the actions of CST on *E. coli*, it could be useful as a therapeutic target for the Gram-negative bacteria that cause many serious infections, including Cholera [45], *E. coli* [46], *Yersinia* [47], *Campylobacter* [48], *Legionella* [49], *Salmonella* [50], *Klebsiella* [51], *Pseudomonas* [52], *Francisella tularensis* [53], *Salmonella typhi* [54], and microbes associated with drug resistance [55–57], and CST might be used as a therapeutic target for the above diseases.

3. Antifungal and Anti-Yeast Effects of CST

3.1. Inhibition of Growth of Fungus and Yeast by CST

Fungal infections are common on the surface of skin, nails, or mucous membranes (superficial or mucocutaneous), underneath the skin (subcutaneous), or in the lungs, brain, or heart (deep infection). Deep fungal infections include Histoplasmosis [58], Coccidioidomycosis (Valley fever) [59], Blastomycosis [60], Aspergillosis [61], Candidal urinary tract infection [62], invasive candidiasis [63,64], *Pneumocystis pneumonia* [65], Mucormycosis [66,67], and Cryptococcosis [68,69]. It is becoming increasingly evident that resistance to antifungal therapy is on the rise [70,71], which calls for the development of alternative therapy for these infections. Host-defense peptides are emerging as new promising candidates to counteract antifungal resistance [72]. To this end, Metz-Boutigue's group tested the effects of CST on the growth of fungus and yeasts. They found MIC values of CST or its human variants ranging from 0.2 μ M to 75 μ M against a host of fungal species (*Neurospora crassa*, *Aspergillus fumigatus*, *A. niger*, *Nectria haematococca*, *Fusarium culmorum*, *F. oxysporum*, *Trichophyton mentagrophytes*, and *T. rubrum*) [21,24] (Figure 3). The MIC₁₀₀ values of CST or its human variants against the above fungal species ranged from 0.8 μ M to 100 μ M [21,24] (Figure 3). CST and its human variants also displayed similar inhibitory effects on the growth of yeasts, with MIC ranging from 1.2 μ M to >240 μ M (Figure 3) [21,24]. The MIC₁₀₀ of CST and its variants against the above yeasts ranged from 6 μ M to 75 μ M [21,24] (Figure 4). Similar to the effects of retro-inverso (RI)-CST (Amino-lqpGpGrfGyararfslkmss-carboxyl, with the CST sequence reversed from carboxyl \rightarrow amino, and chirality was inversed from L \rightarrow D) on catecholamine secretion [73], D-CST exhibited comparable inhibitory effects on the growth of yeast compared to L-CST with MIC ranged from 2 μ M to 9.6 μ M [23]. D-CST was also uncovered to be resistant to proteolytic digestion [23,44,74]. Akin to L-CST, D-CST can also be used to develop therapies for drug-resistant microbial infection [75].

Phylum Fungal species	WT-CST bCgA ₃₄₄₋₃₅₈ MIC (μM)	WT-CST bCgA ₃₄₄₋₃₅₈ MIC ₁₀₀ (μM)	WT-CST hCgA ₃₅₂₋₃₇₂ MIC (μM)	WT-CST hCgA ₃₅₂₋₃₇₂ MIC ₁₀₀ (μM)	G364S-CST hCgA ₃₅₂₋₃₇₂ MIC (μM)	G364S-CST hCgA ₃₅₂₋₃₇₂ MIC ₁₀₀ (μM)	P370L-CST hCgA ₃₅₂₋₃₇₂ MIC (μM)	P370L-CST hCgA ₃₅₂₋₃₇₂ MIC ₁₀₀ (μM)
Ascomycota								
<i>Neurospora crassa</i>	1.2	3.2	20	50	3	5	3	10
<i>Aspergillus fumigatus</i>	10	80	20-80	30	10-20	80	10-20	100
<i>Aspergillus niger</i>			20	30	20	30	10	20
<i>Nectria haematococca</i>	0.2	0.8						
<i>Fusarium culmorum</i>	2	8						
<i>Fusarium oxysporum</i>	6	10						
<i>Trichophyton mentagrophytes</i>	4	20						
<i>Trichophyton rubrum</i>			75	75	20		30	

Figure 3. Effects of WT-CST and natural human variants of CST (Gly364Ser and Pro370Leu) on the growth of fungal species showing MIC and MIC₁₀₀ of CST.

Yeast species	WT-L-CST bCgA ₃₄₄₋₃₅₈ MIC (μM)	WT-L-CST bCgA ₃₄₄₋₃₅₈ MIC ₁₀₀ (μM)	WT-D-CST bCgA ₃₄₄₋₃₅₈ MIC (μM)	WT-L-CST bCgA ₃₄₄₋₃₆₄ MIC (μM)	WT-CST hCgA ₃₅₂₋₃₇₂ MIC (μM)	WT-CST hCgA ₃₅₂₋₃₇₂ MIC ₁₀₀ (μM)	G364S-CST hCgA ₃₅₂₋₃₇₂ MIC ₁₀₀ (μM)	P370L-CST hCgA ₃₅₂₋₃₇₂ MIC ₁₀₀ (μM)
<i>Candida albicans</i> ATCC 14053						50-75	30	30
<i>Candida albicans</i>	1.2	8						
<i>Candida albicans</i> "S"	7.9		5.5	30	>240			
<i>Candida albicans</i> "R"	9.6		9.6	50	>240			
<i>Candida tropicalis</i>	1.8	10						
<i>Candida tropicalis</i> "S"	9.8		8.1	50	>240			
<i>Candida tropicalis</i> "R"	2.0		2.0	20	>240			
<i>Candida glabrata</i>	8	30						
<i>Candida glabrata</i> "S"	38.2	13.4						
<i>Candida glabrata</i> "R"	61.4	15.0		>100	>240			
<i>Candida neoformans</i>	1.4	6		>100	>240			

Figure 4. Effects of WT-CST and natural human variants of CST (Gly364Ser and Pro370Leu) on the growth of yeast species showing MIC and MIC₁₀₀ of CST.

3.2. Mechanisms Underlying the Antifungal and Antiyeast Activities of CST

The composition of fungal cell membranes is similar to that of bacteria, comprising zwitterionic and anionic phospholipids. In contrast, the fungal cell wall is composed of chitin, glucan, ergosterol, and mannoprotein, which reside on the surface of the cytoplasmic membrane. Because of the negative charge on the cytoplasmic membrane, CST could exert its anti-fungal activities in a similar way to its antibacterial activity. Metz-Boutigue's group used confocal laser microscopy to analyze the interaction of the synthetic rhodamine-labeled cateslytin (bCgA_{344-358R}) with fungal (*A. fumigatus*) and yeast (*C. albicans*) membranes [21]. Rhodaminated cateslytin (1 μM) was detected in the inner compartment after 2 min of incubation, implicating rapid and efficient penetration through the cell wall [21]. Using time-lapse video microscopy of fungal growth, they have shown that rhodaminated cateslytin blocked the growth and development of nascent fungus [21]. Penetration of rhodaminated cateslytin takes place at both ends of the small fungi (three cells and expressing a slow growth rate) as compared to larger fungi with a higher growth rate where penetration takes place at one end [21]. Sequence homology of the well-known cell-permeable peptide penetratin with CST representing seven mammalian orders (Primates, Rodentia, Artiodactyla, Perissodactyla, Carnivora, Cetacea, and Monotremata) revealed 63.64% to 75% similarity, which should qualify CST as a cell-permeable peptide (Figure 5).

Common Name	Scientific Name	Order	Sequence	Identity	Similarity
Penetratin			R Q I K I W F Q N R R		
Consensus mammalian CST			R S M K L S F R A R	40%	70%
Human	<i>Homo sapiens</i>	Primates	M K L S F R A R	37.5%	75%
House mouse	<i>Mus musculus</i>	Rodentia	R S M K L S F R T R	40%	70%
Cattle	<i>Bos taurus</i>	Artiodactyla	R S M R L S F R A R	30%	70%
Pig	<i>Sus scrofa</i>	Artiodactyla	R S M K L S F R	37.5%	75%
Horse	<i>Equus caballus</i>	Perissodactyla	R S M K L S F R A R	40%	70%
Walrus	<i>Odobanus rosmarus divergens</i>	Carnivora	R S M K L S F R A R	40%	70%
Killer whale	<i>Orcinus orca</i>	Cetacea	R A M K L S F R A R	40%	70%
Platypus	<i>Ornithorhynchus anatinua</i>	Monotremata	R S M K L S F K T H K	27%	64%

Identical: Black; Similar: Blue; Not Similar: Red

Figure 5. Homology between cell permeable peptide penetratin and CST in seven mammalian orders.

4. CST Regulation of Gut Microbiota

4.1. Microbiomes in Colonic Mucosa versus Feces

Recent studies have identified a larger role of gut microbiota in gut-immune homeostasis and in intestinal pathology. The human intestinal microbiota is dominated by five phyla: high-abundant (>80%) (1) Bacillota (aka Firmicutes) and (2) Bacteroidota; less-abundant (3) Actinomycetota (aka Actinobacteria), (4) Pseudomonadota (aka Proteobacteria), and (5) Verrucomicrobiota [76] as compared to four phyla in mice: high-abundant Bacteroidota, Bacillota, Deferribacterota, and Pseudomonadota [77]; and (4) low-abundant Actinomycetota and Verrucomicrobiota compared to humans. In mouse colonic mucosa samples, 19 phyla were identified [78] (Figure 6). Although CST failed to alter bacterial populations in the four high-abundant phyla, it altered colonic mucosa-associated bacterial community composition at lower taxonomic levels, including orders Bacteroidales, Clostridiales, and YS2, and Families Chitinophagaceae, Clostridiaceae, Coriobacteriaceae, Pseudomonadaceae, Rikenellaceae, and Ruminococcaceae [78]. While CST increased the relative abundance of Bacteroidota, it caused a marked decrease in the Bacillota population (Figure 6). *Bacteroides* and *Parabacteroides* species, representing ~25% of the colonic microbiota, transform simple and complex sugars into volatile short-chain fatty acids (SCFAs), such as acetate, butyrate, and propionate [79–81], which are absorbed in the colon as a nutrient [82,83]. In addition to colonic nutrients, SCFAs are well established for their roles in accelerating gut transit time via the release of serotonin [84,85]. SCFAs also release glucagon-like peptide 1 from the enteroendocrine L-cells [86–88] and improve insulin sensitivity [89–91]. *Bacteroides thetaiotaomicron* produces significant amounts of glycosylhydrolases, which prevent obesity [92]. Other *Bacteroides* species are also reported to prevent obesity and increase insulin sensitivity [93,94]. Furthermore, *Bacteroides fragilis* produces zwitterionic polysaccharide, which activates CD4⁺ T cells to produce interleukin 10 (IL-10). IL-10 plays crucial roles in preventing abscess formation and other unchecked inflammatory responses [95,96]. The functional correlation between different CST mutants across species and their respective microbiota has remained elusive.

	WT Mucosal samples	WT+Sal Fecal samples	WT+CST Fecal samples	CST-KO+Sal Fecal samples	CST-KO+CST Fecal samples	WT+FMT-CST-KO Fecal samples	CST-KO+FMT-WT Fecal samples
Major Phyla (>1%)	Bacillota (aka Firmicutes)	Bacillota	Bacillota ↓	Bacillota	Bacillota ↓↓	Bacillota	Bacillota
	Bacteroidota	Bacteroidota	Bacteroidota ↑↑	Bacteroidota	Bacteroidota ↑	Bacteroidota ↑	Bacteroidota ↓
	Deferribacterota	Deferribacterota	Deferribacterota	Deferribacterota	Deferribacterota	Deferribacterota	Deferribacterota
	Pseudomonadota (aka Proteobacteria)	Pseudomonadota	Pseudomonadota ↑	Pseudomonadota	Pseudomonadota ↑	Pseudomonadota	Pseudomonadota
Minor Phyla (<1%)	Actinomycetota (aka Actinobacteria)	Actinomycetota	Actinomycetota	Actinomycetota	Actinomycetota	Actinomycetota ↑	Actinomycetota
	Parcubacteria (aka OD1)	Parcubacteria	Parcubacteria ↑	Parcubacteria	Parcubacteria	Parcubacteria ↑	Parcubacteria
	Saccharibacteria (aka TM7)	Saccharibacteria			Saccharibacteria	Saccharibacteria	Saccharibacteria
		Campylobacterota	Campylobacterota	Campylobacterota	Campylobacterota	Campylobacterota	Campylobacterota
	Cyanobacteria	Cyanobacteria	Cyanobacteria	Cyanobacteria	Cyanobacteria	Cyanobacteria	Cyanobacteria
		Desulfobacterota	Desulfobacterota ↑	Desulfobacterota	Desulfobacterota	Desulfobacterota	Desulfobacterota
	Fibrobacterota	Fibrobacterota			Fibrobacterota	Fibrobacterota	Fibrobacterota
	Mycoplasmata (aka Tenericutes)	Mycoplasmata			Mycoplasmata	Mycoplasmata	Mycoplasmata
Verrucomicrobiota	Verrucomicrobiota	Verrucomicrobiota	Verrucomicrobiota ↓	Verrucomicrobiota ↑↑	Verrucomicrobiota ↓	Verrucomicrobiota	

Figure 6. Abundance of bacterial species in mucosal and fecal samples in WT and CST-KO mice in presence or absence of CST as well as after fecal microbial transplant. Green arrows indicate CST effects; red arrows indicate FMT effects.

4.2. Microbiomes in CST Knockout (CST-KO) Mice and Inflammation

CST knockout (CST-KO) mice were generated in 2018 and are: insulin-resistant on a normal chow diet [97], hyperadrenergic [98], hypertensive [98], and with a leaky gut [99]. The microbiome in CST-KO mice was found to be quite different in composition than its WT littermates [99]. Microbial richness revealed a significant decrease in CST-KO compared to WT mice [100]. (Figure 7). Surprisingly, Verrucomicrobiota population was very low in CST-KO mice, indicating low levels of *Akkermansia* species. Since *A. muciniphila* modulates obesity by regulating metabolism and energy homeostasis to improve insulin sensitivity and glucose homeostasis [101], low Verrucomicrobiota population possibly contributed to the insulin resistance reported for CST-KO mice [97].

4.3. Alteration of Diversity and Composition of the Microbiota in the CST-KO after Supplementation with CST

Decreased amplicon sequence variants and abundance-based coverage estimator indices in CST-KO mice were restored after supplementation with CST for 15 days [100]. Akin to richness scores, supplementation of CST-KO mice with CST increased the diversity index as assessed by Shannon's *H* and inverted Simpson's index [100]. At the phylum level, CST decreased Bacillota phylum and increased Bacteroidota, Patescibacteria, Desulfobacterota, Verrucomicrobiota, and Proteobacteria in both CST-KO and WT mice [100]. In contrast, CST increased *Alistipes*, *Akkermansia*, and *Roseburia* genera only in CST-KO mice [100].

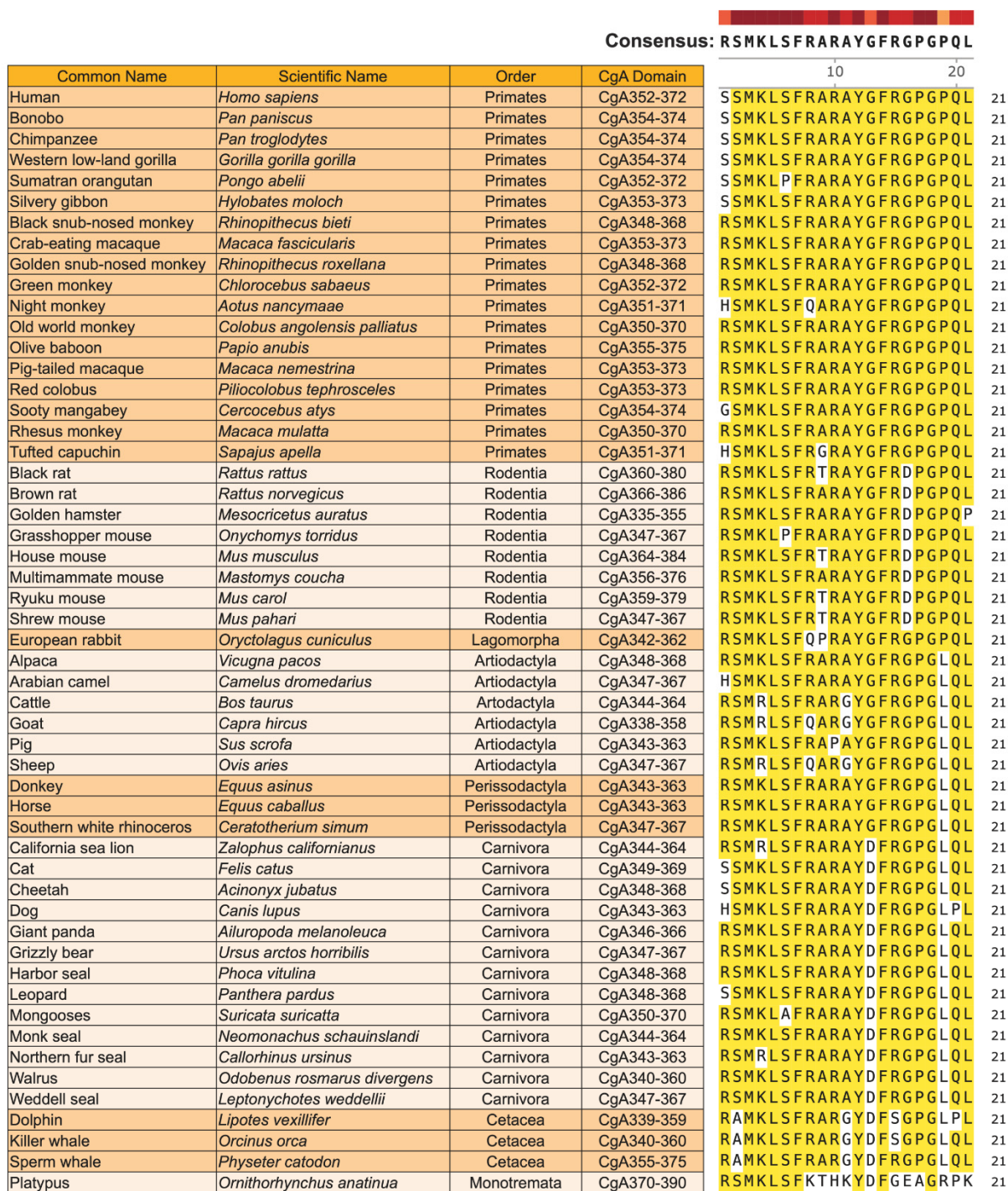


Figure 7. Homology of CST sequence in 53 mammalian species belonging to eight orders. CST sequences were aligned using the MUSCLE method provided by SnapGene software from the following mammalian species: human (*Homo sapiens*: NM_001275), bonobo (*Pan paniscus*: XP_008956465.1), chimpanzee (*Pan troglodytes*: PNI97600.1), western low-land gorilla (*Gorilla gorilla gorilla*: XM_019009788.2), Sumatran orangutan (*Pongo abelii*: XM_002825045.3), silvery gibbon (*Hylobates moloch*: XP_031990963.1), black snub-nosed monkey (*Rhinopithecus bieti*: XM_017857899.1), crab-eating macaque (*Macaca fascicularis*: XP_045252830.1), golden snub-nosed monkey (*Rhinopithecus roxellana*: XM_010384506.1), green monkey (*Chlorocebus sabaenus*: XM_007987644.2), night monkey (*Aotus nancymaae*: XM_012455409.1), old world monkey (*Colobus angolensis palliatus*: XM_011949380.1), olive baboon (*Papio Anubis*: XM_031667888.1), pig-tailed macaque (*Macaca nemestrina*: XM_011717182.1), red colobus (*Piliocolobus tephrosceles*:

XM_023205512.3), Sooty mangabey (*Cercocebus atys*: XM_012083744.1), rhesus monkey (*Macaca mulatta*: NM_001278450.1), tufted capuchin (*Sapajus apella*: XM_032287580.1), black rat (*Rattus rattus*: XM_032908276.1), brown rat (*Rattus norvegicus*: XM_032908276.1), golden hamster (*Mesocricetus auratus*: XM_005068386.4), grasshopper mouse (*Onychomys torridus*: XM_036206345.1), house mouse (*Mus musculus*: NM_007693.2), multimammate mouse (*Mastomys coucha*: XM_031357132.1), Ryuku mouse (*Mus caroli*: XM_021179357.1), Shrew mouse (*Mus pahari*: XM_021202342.2), European rabbit (*Oryctolagus cuniculus*: XM_051826432.1), alpaca (*Vicugna pacos*: XP_031534667.1), Arabian camel (*Camelus dromedarius*: XM_031454226.1), cattle (*Bos taurus*: NM_181005.2), goat (*Capra hircus*: XM_018066172.1), pig (*Sus scrofa*: NP_001157477.2), sheep (*Ovis aries*: XP_004018008.3), donkey (*Equus asinus*: XP_014687627.1), horse (*Equus caballus*: NP_001075283.2), southern white rhinoceros (*Ceratotherium simum*: XP_004434274.1), California sea lion (*Zalophus californianus*: XP_027424506.2), cat (*Felis catus*: XP_023111743.1), cheetah (*Acinonyx jubatus*: XP_026922275.1), dog (*Canis lupus*: XP_038528993.1), giant panda (*Ailuropoda melanoleuca*: XP_019660005.1), grizzly bear (*Ursus arctos horribilis*: XP_048075839.1), harbor seal (*Phoca vitulina*: XP_032261715.1), leopard (*Panthera pardus*: XP_019317643.2), mongooses (*Suricata suricatta*: XP_029807749.1), monk seal (*Neomonachus schauinslandi*: XP_021535325.1), Northern fur seal (*Callorhinus ursinus*: XP_025726236.1), walrus (*Odobenus rosmarus divergens*: XP_004394547.1), weddell-seal (*Leptonychotes weddellii*: XP_030873380.1), dolphin (*Lipotes vexillifer*: XP_007454783.1), killer whale (*Orcinus orca*: XP_004262400.1), sperm whale (*Physeter catodon*: XP_023986851.1), and platypus (*Ornithorhynchus anatinus*: XP_039767777.1). Yellow shows an amino acid match between species.

4.4. Restoration of Microbial Dysbiosis in CST-KO Mice after Fecal Microbial Transplant (FMT) from WT Donor Mice

FMT is now established as an effective therapeutic modality in the treatment of the following diseases: (i) antibiotic-refractory recurrent *Clostridium difficile* colitis with a success rate of up to 95% [102–105], (ii) constipation, (iii) irritable bowel syndrome, and (iv) inflammatory bowel disease [106–108]. Therefore, attempts were made recently to assess whether gut microbial population in mice can be reversed by reciprocal FMT. WT mice that received FMT from the CST-KO mice (WT^{FMT-CST-KO}) encompassed a reduction of Clostridia and *Akkermansia* [109], which are linked to metabolic disorders and insulin resistance [110,111] and a marked increase in the Proteobacteria population, which are associated with active inflammatory bowel disease (IBD) states [112,113]. Of note, CST-KO mice are insulin-resistant on a normal chow diet [97]. In contrast, insulin-resistant CST-KO mice that received FMT from the WT mice (CST-KO^{FMT-WT}) showed an increase in richness, a notable reduction of *Staphylococcus*, and an increase in the butyrate-producing *Intestinimonas* [109] (Figure 6). Butyrate, taken up directly by colonocytes, serves not only as a direct source of energy that contributes directly to a healthy gut, but also acts as a signaling molecule that affects many factors such as satiety, secretion of hormones, and glucose metabolism [114–116]. Furthermore, reduced levels of butyrate are strongly associated with IBD and metabolic disorders [117,118]. Butyrate has also been shown to restore gut barrier integrity [119], modulates regulatory T cell function [120–122], and regulates certain serine proteases [123,124].

5. Catestatin and Innate Immunity

The first indication for the role of CST in innate immunity came from a study in rats where intravenous administration of CST was shown to reduce pressor responses by electrical stimulation [125]. The hypotensive effect of CST was revealed to be mediated at least in part by profuse histamine release (by ~21-fold) and action at the H₁ receptor [125]. The *in vivo* studies were later confirmed in peritoneal and pleural mast cells where CST caused dose-dependent release of histamine utilizing signaling pathways established for wasp venom peptide mastoparan and other amphiphilic cationic neuropeptides (the peptidergic pathway) [126]. This pathway is in sharp contrast to the nicotinic-cholinergic pathway used by CST to induce catecholamine secretion from chromaffin cells [5]. Subsequent studies uncover the following: (i) release of immunoreactive CST-containing peptides from

human stimulated polymorphonuclear neutrophils [21]; (ii) detection of CST in mouse peritoneal macrophages by Western blots [98]; (iii) detection of CST in human monocytes and monocyte-derived macrophages by Western blots [127]; (iv) blockade of lipopolysaccharide (LPS)-induced increase in expression of tumor necrosis factor alpha [127]; (v) decreased expression of proinflammatory cytokines by CST in plasma and heart [98]; (vi) inhibition of infiltration of macrophages in obese liver [97]; (vii) degranulation of primary mast cells from human peripheral blood [128]; and (viii) low plasma CST in fatal COVID-19 patients [129]. These findings implicate CST as an immunomodulatory peptide. Since receptor-ligand interactions are an essential driver of host-immune response [130], it is important to examine if CST can bind with a receptor on immune cells and regulate their polarization and function in host defense.

6. Evolutionary Conservation and Selection Pressure on CST in Mammals

6.1. Homology of CST in Mammals

Sequence alignment of CST in 53 mammalian species belonging to eight orders revealed >80% homology in 52 species, except in Platypus (lowest in the mammalian phylogenetic tree) where the homology with the primates (highest in the mammalian phylogenetic tree) was >58% (Figure 7), indicating that CST is highly conserved in mammals. The homology of individual amino acids is summarized in Figure 8. Aromatic amino acids such as phenylalanine, tyrosine and tryptophan are reported to exhibit a rigid, planar structure and possess added stability due to the π -electron cloud situated above and below the plane of the aromatic ring [131–133]. Therefore, F₇, Y₁₂, F₁₄ conserved residues in CST can undergo aromatic–aromatic interactions such as hydrogen bonding coupled with attractive, non-covalent, dipole, and van der Waals interactions, and also pi-stacking of the benzene rings [134–137]. These interactions, in turn, can stabilize the overall structure of CST, as reported earlier for other proteins [138–141]. Analysis of the energetics of protein analyses revealed that the packing of non-polar groups in the protein interior is favorable owing to the favorable enthalpy of van der Waals interactions [142]. Therefore, it is reasonable to assume that van der Waals interactions of the aromatic amino acids (F₇, Y₁₂, F₁₄) in association with van der Waals interactions of apolar (L₅, G₁₈) amino acids provided a global stability for CST [143,144]. In the course of evolution, with the change in interacting partners across species, we see a significant reduction in the conservation of charged residue. Interestingly, for the maintenance of structural framework, a 100% conservation of hydrophobic amino acid is maintained across the species through the mammalian evolutionary ladder.

6.2. Single Nucleotide Polymorphisms (SNPs) in the CST Domain of Mammals

Four non-synonymous SNPs have been identified in CST domain of CgA: Gly₃₆₄Ser (US, Indian, and Japanese populations) [22,145,146], Gly₃₆₇Val (only in Indian populations) [145], Pro₃₇₀Leu (US and Indian populations) [22], and Arg₃₇₄Gln (US populations only) [22]. Pro₃₇₀Leu-CST has the highest potency of inhibiting catecholamine secretion and desensitizing catecholamine secretion, followed by WT-CST and Gly₃₆₄Ser-CST [22]. As a sharp contrast to catecholamine secretion [22], Gly₃₆₄Ser was reported to be two-times more effective than Pro₃₇₀Leu in exerting antibacterial activities [21].

R	S	M	K	L	S	F
1 h352	2 h353	3 h354	4 h355	5 h356	6 h357	7 h358
73%	>94%	100%	>90%	100%	>92%	100%
R	A	R	A	Y	G	F
8 h359	9 h360	10 h361	11 h362	12 h363	13 h364	14 h365
>92%	>86%	>96%	>86%	100%	>66%	100%
R	G	P	G	P	Q	L
15 h366	16 h367	17 h368	18 h369	19 h370	20 h371	21 h372
>94%	>83%	>98%	100%	>58%	>94%	>96%

Consensus sequence
 Amino Acid number
 Homology

Figure 8. Homology of the individual amino acid in catestatin sequence in 53 mammalian species belonging to seven orders.

7. Conclusions

(i) High conservation of CST in mammals: Alignment of CST sequences from 53 mammalian species belonging to eight orders revealed that CST sequence is highly conserved (>90% in 90% species) in mammals: Five (~24%) amino acids (M₃, L₅, F₇, F₁₄, and G₁₈) are 100% conserved; nine (~43%) amino acids (S₂, K₄, S₆, R₈, R₁₀, R₁₅, P₁₇, Q₂₀ and L₂₁) are 90–96% conserved; and three (~14%) amino acids (A₉, A₁₁, and G₁₆) are >80% conserved. The least conserved sequences are G₁₃ (>66%) and P₁₉ (>58%), where human variants of CST were reported for G₁₃ (G₁₃S) and P₁₉ (P₁₉L), indicating that natural selection pressures still exist on those two amino acids [147–150].

(ii) CST as an immunomodulatory peptide: Existing literature (expression of CST in innate immune cells [21,98,127,151], inhibition of macrophage infiltration in tissues [97–99], decreased expression of pro-inflammatory cytokines by CST [97,98], and low plasma CST in fatal COVID-19 patients [129]) implicate CST as an immunomodulatory peptide.

(iii) CST as an antimicrobial peptide: Prominent effects of CST in the low micromolar range on inhibition of growth of Gram-positive and Gram-negative bacteria, fungi, and yeast establish CST as an antimicrobial peptide [21].

(iv) D-bCST_{1–15} as a potential therapy for microbial infection: D-bCST_{1–15} could be used as a monotherapy or as a combination therapy with cefotaxime, amoxicillin, and methicillin against the “superbugs” because it has more effective antibacterial activity compared to L-bCST_{1–15}, penetration through the bacterial cell wall, resistance to bacterial proteases, undetectable susceptibility to resistance, and potentiation/synergic action of commonly prescribed antibiotics [23].

(v) CST as a cell permeable peptide: Penetration of CST (pI 12.03–12.48) in bacteria, fungus, yeast, and neutrophils [21,152], coupled with 70–75% homology with cell penetrating peptide Penetratin (pI 12.62), rightfully qualify CST as a cell permeable peptide.

(vi) Gut microbiome-mediated improvement in insulin sensitivity by CST: The increased ratio of *Bacilotta* to *Bacteroidota*, together with low levels of *Verrucomicrobiota* (e.g., *Akkermansia* spp.) in CST-KO mice [100], not only explains insulin resistance in CST-KO mice [97] but also implicates that CST is necessary for the maintenance of insulin sensitivity. A decreased ratio of *Bacilotta* to *Bacteroidota* coupled with increased abundance of *Verrucomicrobiota* after supplementation of CST-KO mice with CST [100] confirm that CST is necessary and sufficient to increase insulin sensitivity by modulating gut microbiota. Decreased population of *Akkermansia* and increased population of Proteobacteria in WT^{FMT}-CST-KO coupled with increased population of butyrate producing *Intestimonas* in CST-KO^{FMT-WT} [109] further substantiates regulation of obesity and insulin resistance by CST [97] via regulation of gut microbial population [100,109].

(vii) Improvement in antimicrobial effect of CST by cyclization: Based on the existing literature [39,41], we propose that cyclization of CST would markedly improve the antibacterial activity of CST.

Author Contributions: S.K.M. conceived the idea and wrote major portion of the manuscript. S.M. made all the figures. S.J., S.M., S.D., S.C. and S.K.M. performed literature search, interpreted data, and wrote the manuscript. All authors have read and agreed to the published version of the manuscript.

Funding: This research was supported by grants from the National Institutes of Health (1 R21 AG072487-01 and 1 R21 AG080246-01 to S.K.M.). S.J. is supported by AFTD Holloway Postdoctoral Fellowship (Award #2020-02).

Institutional Review Board Statement: Not applicable.

Informed Consent Statement: Not applicable.

Data Availability Statement: Not applicable.

Conflicts of Interest: S.K.M. is a co-inventor of a patent on CST regulation of obesity.

References

- Zasloff, M. Antimicrobial peptides of multicellular organisms. *Nature* **2002**, *415*, 389–395. [[CrossRef](#)] [[PubMed](#)]
- Winkler, H.; Fischer-Colbrie, R. The Chromogranins A and B: The first 25 years and future perspectives. *Neuroscience* **1992**, *49*, 497–528. [[CrossRef](#)] [[PubMed](#)]
- Montero-Hadjadje, M.; Vaingankar, S.; Elias, S.; Tostivint, H.; Mahata, S.K.; Anouar, Y. Chromogranins A and B and secretogranin II: Evolutionary and functional aspects. *Acta Physiol. (Oxf.)* **2008**, *192*, 309–324. [[CrossRef](#)] [[PubMed](#)]
- Bartolomucci, A.; Possenti, R.; Mahata, S.K.; Fischer-Colbrie, R.; Loh, Y.P.; Salton, S.R. The extended granin family: Structure, function, and biomedical implications. *Endocr. Rev.* **2011**, *32*, 755–797. [[CrossRef](#)]
- Mahata, S.K.; O'Connor, D.T.; Mahata, M.; Yoo, S.H.; Taupenot, L.; Wu, H.; Gill, B.M.; Parmer, R.J. Novel autocrine feedback control of catecholamine release. A discrete Chromogranin A fragment is a noncompetitive nicotinic cholinergic antagonist. *J. Clin. Investig.* **1997**, *100*, 1623–1633. [[CrossRef](#)]
- Mahata, S.K.; Corti, A. Chromogranin A and its fragments in cardiovascular, immunometabolic, and cancer regulation. *Ann. N. Y. Acad. Sci.* **2019**, *1455*, 34–58. [[CrossRef](#)]
- Taylor, C.V.; Taupenot, L.; Mahata, S.K.; Mahata, M.; Wu, H.; Yasothornsrikul, S.; Toneff, T.; Caporale, C.; Jiang, Q.; Parmer, R.J.; et al. Formation of the catecholamine release-inhibitory peptide catestatin from Chromogranin A. Determination of proteolytic cleavage sites in hormone storage granules. *J. Biol. Chem.* **2000**, *275*, 22905–22915. [[CrossRef](#)]
- Parmer, R.J.; Mahata, M.; Gong, Y.; Mahata, S.K.; Jiang, Q.; O'Connor, D.T.; Xi, X.-P.; Miles, L.A. Processing of Chromogranin A by plasmin provides a novel mechanism for regulating catecholamine secretion. *J. Clin. Investig.* **2000**, *106*, 907–915. [[CrossRef](#)]
- Jiang, Q.; Taupenot, L.; Mahata, S.K.; Mahata, M.; O'Connor, D.T.; Miles, L.A.; Parmer, R.J. Proteolytic cleavage of Chromogranin A (CgA) by plasmin: Selective liberation of a specific bioactive CgA fragment that regulates catecholamine release. *J. Biol. Chem.* **2001**, *276*, 25022–25029. [[CrossRef](#)]
- Lee, J.C.; Taylor, C.V.; Gaucher, S.P.; Toneff, T.; Taupenot, L.; Yasothornsrikul, S.; Mahata, S.K.; Sei, C.; Parmer, R.J.; Neveu, J.M.; et al. Primary sequence characterization of catestatin intermediates and peptides defines proteolytic cleavage sites utilized for converting Chromogranin A into active catestatin secreted from neuroendocrine chromaffin cells. *Biochemistry* **2003**, *42*, 6938–6946. [[CrossRef](#)]
- Biswas, N.; Vaingankar, S.M.; Mahata, M.; Das, M.; Gayen, J.R.; Taupenot, L.; Torpey, J.W.; O'Connor, D.T.; Mahata, S.K. Proteolytic cleavage of human Chromogranin A containing naturally occurring catestatin variants: Differential processing at catestatin region by plasmin. *Endocrinology* **2008**, *149*, 749–757. [[CrossRef](#)] [[PubMed](#)]

12. Biswas, N.; Rodriguez-Flores, J.L.; Courel, M.; Gayen, J.R.; Vaingankar, S.M.; Mahata, M.; Torpey, J.W.; Taupenot, L.; O'Connor, D.T.; Mahata, S.K. Cathepsin L Co-Localizes with Chromogranin A in Chromaffin Vesicles to Generate Active Peptides. *Endocrinology* **2009**, *150*, 3547–3557. [[CrossRef](#)] [[PubMed](#)]
13. Mahata, S.K.; Mahata, M.; Parmer, R.J.; O'Connor, D.T. Desensitization of catecholamine release: The novel catecholamine release-inhibitory peptide catestatin (Chromogranin A_{344–364}) acts at the receptor to prevent nicotinic cholinergic tolerance. *J. Biol. Chem.* **1999**, *274*, 2920–2928. [[CrossRef](#)] [[PubMed](#)]
14. Taupenot, L.; Mahata, S.K.; Mahata, M.; Parmer, R.J.; O'Connor, D.T. Interaction of the catecholamine release-inhibitory peptide catestatin (human Chromogranin A(352–372)) with the chromaffin cell surface and Torpedo electroplax: Implications for nicotinic cholinergic antagonism. *Regul. Pept.* **2000**, *95*, 9–17. [[CrossRef](#)] [[PubMed](#)]
15. Mahata, S.K.; Mahata, M.; Wakade, A.R.; O'Connor, D.T. Primary structure and function of the catecholamine release inhibitory peptide catestatin (Chromogranin A_{344–364}): Identification of amino acid residues crucial for activity. *Mol. Endocrinol.* **2000**, *14*, 1525–1535. [[PubMed](#)]
16. Preece, N.E.; Nguyen, M.; Mahata, M.; Mahata, S.K.; Mahapatra, N.R.; Tsigelny, I.; O'Connor, D.T. Conformational preferences and activities of peptides from the catecholamine release-inhibitory (catestatin) region of Chromogranin A. *Regul. Pept.* **2004**, *118*, 75–87. [[CrossRef](#)]
17. Mahata, S.K. Catestatin—The catecholamine release inhibitory peptide: A structural and functional overview. *Curr. Med. Chem. Immun. Endoc. Metab. Agents* **2004**, *4*, 221–234. [[CrossRef](#)]
18. Mahapatra, N.R.; Mahata, M.; Mahata, S.K.; O'Connor, D.T. The Chromogranin A fragment catestatin: Specificity, potency and mechanism to inhibit exocytotic secretion of multiple catecholamine storage vesicle co-transmitters. *J. Hypertens.* **2006**, *24*, 895–904. [[CrossRef](#)]
19. Mahata, S.K.; Mahata, M.; Fung, M.M.; O'Connor, D.T. Catestatin: A multifunctional peptide from Chromogranin A. *Regul. Pept.* **2010**, *162*, 33–43. [[CrossRef](#)]
20. Mahata, S.K.; Kiranmayi, M.; Mahapatra, N.R. Catestatin: A Master Regulator of Cardiovascular Functions. *Curr. Med. Chem.* **2018**, *25*, 1352–1374. [[CrossRef](#)]
21. Briolat, J.; Wu, S.D.; Mahata, S.K.; Gonthier, B.; Bagnard, D.; Chasserot-Golaz, S.; Helle, K.B.; Aunis, D.; Metz-Boutigue, M.H. New antimicrobial activity for the catecholamine release-inhibitory peptide from Chromogranin A. *Cell. Mol. Life Sci.* **2005**, *62*, 377–385. [[CrossRef](#)] [[PubMed](#)]
22. Wen, G.; Mahata, S.K.; Cadman, P.; Mahata, M.; Ghosh, S.; Mahapatra, N.R.; Rao, F.; Stridsberg, M.; Smith, D.W.; Mahboubi, P.; et al. Both rare and common polymorphisms contribute functional variation at CHGA, a regulator of catecholamine physiology. *Am. J. Hum. Genet.* **2004**, *74*, 197–207. [[CrossRef](#)] [[PubMed](#)]
23. Zaet, A.; Dartevelle, P.; Daouad, F.; Ehlinger, C.; Quiles, F.; Francius, G.; Boehler, C.; Bergthold, C.; Frisch, B.; Prevost, G.; et al. D-Cateslytin, a new antimicrobial peptide with therapeutic potential. *Sci. Rep.* **2017**, *7*, 15199. [[CrossRef](#)]
24. Radek, K.A.; Lopez-Garcia, B.; Hupe, M.; Niesman, I.R.; Elias, P.M.; Taupenot, L.; Mahata, S.K.; O'Connor, D.T.; Gallo, R.L. The neuroendocrine peptide catestatin is a cutaneous antimicrobial and induced in the skin after injury. *J. Investig. Dermatol.* **2008**, *128*, 1525–1534. [[CrossRef](#)] [[PubMed](#)]
25. Scheffers, D.J.; Pinho, M.G. Bacterial cell wall synthesis: New insights from localization studies. *Microbiol. Mol. Biol. Rev.* **2005**, *69*, 585–607. [[CrossRef](#)] [[PubMed](#)]
26. Brown, A.R.; Gordon, R.A.; Hyland, S.N.; Siegrist, M.S.; Grimes, C.L. Chemical Biology Tools for Examining the Bacterial Cell Wall. *Cell. Chem. Biol.* **2020**, *27*, 1052–1062. [[CrossRef](#)]
27. Lopez-Siles, M.; Corral-Lugo, A.; McConnell, M.J. Vaccines for multidrug resistant Gram negative bacteria: Lessons from the past for guiding future success. *FEMS Microbiol. Rev.* **2021**, *45*, fuaa054. [[CrossRef](#)]
28. Welch, R.A. Pore-forming cytolysins of gram-negative bacteria. *Mol. Microbiol.* **1991**, *5*, 521–528. [[CrossRef](#)]
29. Mahlapuu, M.; Hakansson, J.; Ringstad, L.; Bjorn, C. Antimicrobial Peptides: An Emerging Category of Therapeutic Agents. *Front. Cell. Infect. Microbiol.* **2016**, *6*, 194. [[CrossRef](#)]
30. Lee, T.H.; Hirst, D.J.; Aguilar, M.I. New insights into the molecular mechanisms of biomembrane structural changes and interactions by optical biosensor technology. *Biochim. Biophys. Acta* **2015**, *1848*, 1868–1885. [[CrossRef](#)]
31. Wadhvani, P.; Epand, R.F.; Heidenreich, N.; Burck, J.; Ulrich, A.S.; Epand, R.M. Membrane-active peptides and the clustering of anionic lipids. *Biophys. J.* **2012**, *103*, 265–274. [[CrossRef](#)] [[PubMed](#)]
32. Bogdanov, M.; Pyrshev, K.; Yesylevskyy, S.; Ryabichko, S.; Boiko, V.; Ivanchenko, P.; Kiyamova, R.; Guan, Z.; Ramseyer, C.; Dowhan, W. Phospholipid distribution in the cytoplasmic membrane of Gram-negative bacteria is highly asymmetric, dynamic, and cell shape-dependent. *Sci. Adv.* **2020**, *6*, eaaz6333. [[CrossRef](#)] [[PubMed](#)]
33. Vollmer, W.; Seligman, S.J. Architecture of peptidoglycan: More data and more models. *Trends Microbiol.* **2010**, *18*, 59–66. [[CrossRef](#)] [[PubMed](#)]
34. Rojas, E.R.; Billings, G.; Odermatt, P.D.; Auer, G.K.; Zhu, L.; Miguel, A.; Chang, F.; Weibel, D.B.; Theriot, J.A.; Huang, K.C. The outer membrane is an essential load-bearing element in Gram-negative bacteria. *Nature* **2018**, *559*, 617–621. [[CrossRef](#)] [[PubMed](#)]
35. Percy, M.G.; Grundling, A. Lipoteichoic acid synthesis and function in gram-positive bacteria. *Annu. Rev. Microbiol.* **2014**, *68*, 81–100. [[CrossRef](#)]
36. Bowdish, D.M.; Davidson, D.J.; Hancock, R.E. A re-evaluation of the role of host defence peptides in mammalian immunity. *Curr. Protein. Pept. Sci.* **2005**, *6*, 35–51. [[CrossRef](#)]

37. Sahu, B.S.; Mohan, J.; Sahu, G.; Singh, P.K.; Sonawane, P.J.; Sasi, B.K.; Allu, P.K.; Maji, S.K.; Bera, A.K.; Senapati, S.; et al. Molecular interactions of the physiological anti-hypertensive peptide catestatin with the neuronal nicotinic acetylcholine receptor. *J. Cell Sci.* **2012**, *125*, 2323–2337. [[CrossRef](#)]
38. Tsigelny, I.; Mahata, S.K.; Taupenot, L.; Preece, N.E.; Mahata, M.; Khan, I.; Parmer, R.J.; O'Connor, D.T. Mechanism of action of Chromogranin A on catecholamine release: Molecular modeling of the catestatin region reveals a b-strand/loop/b-strand structure secured by hydrophobic interactions and predictive of activity. *Regul. Pept.* **1998**, *77*, 43–53. [[CrossRef](#)] [[PubMed](#)]
39. Dathe, M.; Nikolenko, H.; Klose, J.; Bienert, M. Cyclization increases the antimicrobial activity and selectivity of arginine- and tryptophan-containing hexapeptides. *Biochemistry* **2004**, *43*, 9140–9150. [[CrossRef](#)]
40. Lazzaro, B.P.; Zasloff, M.; Rolff, J. Antimicrobial peptides: Application informed by evolution. *Science* **2020**, *368*, eaau5480. [[CrossRef](#)]
41. Wessolowski, A.; Bienert, M.; Dathe, M. Antimicrobial activity of arginine- and tryptophan-rich hexapeptides: The effects of aromatic clusters, D-amino acid substitution and cyclization. *J. Pept. Res.* **2004**, *64*, 159–169. [[CrossRef](#)] [[PubMed](#)]
42. Jean-Francois, F.; Castano, S.; Desbat, B.; Odaert, B.; Roux, M.; Metz-Boutigue, M.H.; Dufourc, E.J. Aggregation of cateslytin beta-sheets on negatively charged lipids promotes rigid membrane domains. A new mode of action for antimicrobial peptides? *Biochemistry* **2008**, *47*, 6394–6402. [[CrossRef](#)] [[PubMed](#)]
43. Eppard, R.M.; Eppard, R.F. Lipid domains in bacterial membranes and the action of antimicrobial agents. *Biochim. Biophys. Acta* **2009**, *1788*, 289–294. [[CrossRef](#)]
44. Scavello, F.; Mutschler, A.; Helle, S.; Schneider, F.; Chasserot-Golaz, S.; Strub, J.M.; Cianferani, S.; Haikel, Y.; Metz-Boutigue, M.H. Catestatin in innate immunity and Cateslytin-derived peptides against superbugs. *Sci. Rep.* **2021**, *11*, 15615. [[CrossRef](#)] [[PubMed](#)]
45. Costa, T.R.; Felisberto-Rodrigues, C.; Meir, A.; Prevost, M.S.; Redzej, A.; Trokter, M.; Waksman, G. Secretion systems in Gram-negative bacteria: Structural and mechanistic insights. *Nat. Rev. Microbiol.* **2015**, *13*, 343–359. [[CrossRef](#)] [[PubMed](#)]
46. Bonten, M.; Johnson, J.R.; van den Biggelaar, A.H.J.; Georgalis, L.; Geurtsen, J.; de Palacios, P.I.; Gravenstein, S.; Verstraeten, T.; Hermans, P.; Poolman, J.T. Epidemiology of Escherichia coli Bacteremia: A Systematic Literature Review. *Clin. Infect. Dis.* **2021**, *72*, 1211–1219. [[CrossRef](#)] [[PubMed](#)]
47. Pechous, R.D.; Sivaraman, V.; Stasulli, N.M.; Goldman, W.E. Pneumonic Plague: The Darker Side of Yersinia pestis. *Trends Microbiol.* **2016**, *24*, 190–197. [[CrossRef](#)]
48. Kim, S.H.; Chelliah, R.; Ramakrishnan, S.R.; Perumal, A.S.; Bang, W.S.; Rubab, M.; Daliri, E.B.; Barathikannan, K.; Elahi, F.; Park, E.; et al. Review on Stress Tolerance in Campylobacter jejuni. *Front. Cell. Infect. Microbiol.* **2020**, *10*, 596570. [[CrossRef](#)]
49. Cunha, B.A.; Burillo, A.; Bouza, E. Legionnaires' disease. *Lancet* **2016**, *387*, 376–385. [[CrossRef](#)]
50. Coburn, B.; Grassl, G.A.; Finlay, B.B. Salmonella, the host and disease: A brief review. *Immunol. Cell Biol.* **2007**, *85*, 112–118. [[CrossRef](#)]
51. Lee, G.C.; Burgess, D.S. Treatment of Klebsiella pneumoniae carbapenemase (KPC) infections: A review of published case series and case reports. *Ann. Clin. Microbiol. Antimicrob.* **2012**, *11*, 32. [[CrossRef](#)] [[PubMed](#)]
52. Capatina, D.; Feier, B.; Hosu, O.; Tertis, M.; Cristea, C. Analytical methods for the characterization and diagnosis of infection with Pseudomonas aeruginosa: A critical review. *Anal. Chim. Acta* **2022**, *1204*, 339696. [[CrossRef](#)] [[PubMed](#)]
53. Hennebique, A.; Boisset, S.; Maurin, M. Tularemia as a waterborne disease: A review. *Emerg. Microbes Infect.* **2019**, *8*, 1027–1042. [[CrossRef](#)] [[PubMed](#)]
54. Butler, T. Treatment of typhoid fever in the 21st century: Promises and shortcomings. *Clin. Microbiol. Infect.* **2011**, *17*, 959–963. [[CrossRef](#)]
55. Mazzariol, A.; Bazaj, A.; Cornaglia, G. Multi-drug-resistant Gram-negative bacteria causing urinary tract infections: A review. *J. Chemother.* **2017**, *29*, 2–9. [[CrossRef](#)]
56. Blair, J.M.; Richmond, G.E.; Piddock, L.J. Multidrug efflux pumps in Gram-negative bacteria and their role in antibiotic resistance. *Future Microbiol.* **2014**, *9*, 1165–1177. [[CrossRef](#)]
57. Vasoo, S.; Barreto, J.N.; Tosh, P.K. Emerging issues in gram-negative bacterial resistance: An update for the practicing clinician. *Mayo Clin. Proc.* **2015**, *90*, 395–403. [[CrossRef](#)]
58. Sizemore, T.C. Rheumatologic manifestations of histoplasmosis: A review. *Rheumatol. Int.* **2013**, *33*, 2963–2965. [[CrossRef](#)]
59. Jude, C.M.; Nayak, N.B.; Patel, M.K.; Deshmukh, M.; Batra, P. Pulmonary coccidioidomycosis: Pictorial review of chest radiographic and CT findings. *Radiographics* **2014**, *34*, 912–925. [[CrossRef](#)]
60. Linder, K.A.; Kauffman, C.A.; Miceli, M.H. Blastomycosis: A Review of Mycological and Clinical Aspects. *J. Fungi* **2023**, *9*, 117. [[CrossRef](#)]
61. Mahdavinia, M.; Grammer, L.C. Management of allergic bronchopulmonary aspergillosis: A review and update. *Ther. Adv. Respir. Dis.* **2012**, *6*, 173–187. [[CrossRef](#)]
62. Griffith, N.; Danziger, L. Candida auris Urinary Tract Infections and Possible Treatment. *Antibiotics* **2020**, *9*, 898. [[CrossRef](#)]
63. Ben-Ami, R. Treatment of Invasive Candidiasis: A Narrative Review. *J. Fungi* **2018**, *4*, 97. [[CrossRef](#)]
64. McCarty, T.P.; Pappas, P.G. Invasive Candidiasis. *Infect. Dis. Clin. N. Am.* **2016**, *30*, 103–124. [[CrossRef](#)]
65. de Boer, M.G.; de Fijter, J.W.; Kroon, F.P. Outbreaks and clustering of Pneumocystis pneumonia in kidney transplant recipients: A systematic review. *Med. Mycol.* **2011**, *49*, 673–680.
66. Jeong, W.; Keighley, C.; Wolfe, R.; Lee, W.L.; Slavin, M.A.; Kong, D.C.M.; Chen, S.C. The epidemiology and clinical manifestations of mucormycosis: A systematic review and meta-analysis of case reports. *Clin. Microbiol. Infect.* **2019**, *25*, 26–34. [[CrossRef](#)]

67. Nair, A.G.; Dave, T.V. Transcutaneous retrobulbar injection of amphotericin B in rhino-orbital-cerebral mucormycosis: A review. *Orbit* **2022**, *41*, 275–286. [[CrossRef](#)]
68. Setianingrum, F.; Rautemaa-Richardson, R.; Denning, D.W. *Pulmonary cryptococcosis: A review of pathobiology and clinical aspects.* *Med. Mycol.* **2019**, *57*, 133–150. [[CrossRef](#)]
69. Montoya, M.C.; Magwene, P.M.; Perfect, J.R. Associations between *Cryptococcus* Genotypes, Phenotypes, and Clinical Parameters of Human Disease: A Review. *J. Fungi* **2021**, *7*, 260. [[CrossRef](#)]
70. Bermas, A.; Geddes-McAlister, J. Combatting the evolution of antifungal resistance in *Cryptococcus neoformans*. *Mol. Microbiol.* **2020**, *114*, 721–734. [[CrossRef](#)]
71. Wall, G.; Lopez-Ribot, J.L. Current Antimycotics, New Prospects, and Future Approaches to Antifungal Therapy. *Antibiotics* **2020**, *9*, 445. [[CrossRef](#)] [[PubMed](#)]
72. Buda De Cesare, G.; Cristy, S.A.; Garsin, D.A.; Lorenz, M.C. Antimicrobial Peptides: A New Frontier in Antifungal Therapy. *mBio* **2020**, *11*, e02123–20. [[CrossRef](#)] [[PubMed](#)]
73. Biswas, N.; Gayen, J.; Mahata, M.; Su, Y.; Mahata, S.K.; O'Connor, D.T. Novel peptide isomer strategy for stable inhibition of catecholamine release: Application to hypertension. *Hypertension* **2012**, *60*, 1552–1559. [[CrossRef](#)] [[PubMed](#)]
74. Aslam, R.; Marban, C.; Corazzol, C.; Jehl, F.; Delalande, F.; Van Dorsselaer, A.; Prevost, G.; Haikel, Y.; Taddei, C.; Schneider, F.; et al. Cateslytin, a Chromogranin A derived peptide is active against *Staphylococcus aureus* and resistant to degradation by its proteases. *PLoS ONE* **2013**, *8*, e68993. [[CrossRef](#)] [[PubMed](#)]
75. Mancino, D.; Kharouf, N.; Scavello, F.; Helle, S.; Salloum-Yared, F.; Mutschler, A.; Mathieu, E.; Lavallo, P.; Metz-Boutigue, M.H.; Haikel, Y. The Catestatin-Derived Peptides Are New Actors to Fight the Development of Oral Candidosis. *Int. J. Mol. Sci.* **2022**, *23*, 2066. [[CrossRef](#)]
76. Rios-Covian, D.; Salazar, N.; Gueimonde, M.; de Los Reyes-Gavilan, C.G. Shaping the Metabolism of Intestinal Bacteroides Population through Diet to Improve Human Health. *Front. Microbiol.* **2017**, *8*, 376. [[CrossRef](#)]
77. Rabbi, M.F.; Eissa, N.; Munyaka, P.M.; Kermarrec, L.; Elgazzar, O.; Khafipour, E.; Bernstein, C.N.; Ghia, J.E. Reactivation of Intestinal Inflammation Is Suppressed by Catestatin in a Murine Model of Colitis via M1 Macrophages and Not the Gut Microbiota. *Front. Immunol.* **2017**, *8*, 985. [[CrossRef](#)]
78. Rabbi, M.F.; Munyaka, P.M.; Eissa, N.; Metz-Boutigue, M.H.; Khafipour, E.; Ghia, J.E. Human Catestatin Alters Gut Microbiota Composition in Mice. *Front. Microbiol.* **2016**, *7*, 2151. [[CrossRef](#)]
79. Horvath, T.D.; Ihekweazu, F.D.; Haidacher, S.J.; Ruan, W.; Engevik, K.A.; Fultz, R.; Hoch, K.M.; Luna, R.A.; Oezguen, N.; Spinler, J.K.; et al. *Bacteroides ovatus* colonization influences the abundance of intestinal short chain fatty acids and neurotransmitters. *iScience* **2022**, *25*, 104158. [[CrossRef](#)]
80. Fernandez-Julia, P.J.; Munoz-Munoz, J.; van Sinderen, D. A comprehensive review on the impact of beta-glucan metabolism by *Bacteroides* and *Bifidobacterium* species as members of the gut microbiota. *Int. J. Biol. Macromol.* **2021**, *181*, 877–889. [[CrossRef](#)]
81. Bornet, E.; Westermann, A.J. The ambivalent role of *Bacteroides* in enteric infections. *Trends Microbiol.* **2022**, *30*, 104–108. [[CrossRef](#)] [[PubMed](#)]
82. Wong, J.M.; de Souza, R.; Kendall, C.W.; Emam, A.; Jenkins, D.J. Colonic health: Fermentation and short chain fatty acids. *J. Clin. Gastroenterol.* **2006**, *40*, 235–243. [[CrossRef](#)]
83. Cummings, J.H.; Macfarlane, G.T. Role of intestinal bacteria in nutrient metabolism. *JPEN J. Parenter. Enteral Nutr.* **1997**, *21*, 357–365. [[CrossRef](#)]
84. Reigstad, C.S.; Salmons, C.E.; Rainey, J.F., 3rd; Szurszewski, J.H.; Linden, D.R.; Sonnenburg, J.L.; Farrugia, G.; Kashyap, P.C. Gut microbes promote colonic serotonin production through an effect of short-chain fatty acids on enterochromaffin cells. *FASEB J.* **2015**, *29*, 1395–1403. [[CrossRef](#)] [[PubMed](#)]
85. Ge, X.; Pan, J.; Liu, Y.; Wang, H.; Zhou, W.; Wang, X. Intestinal Crosstalk between Microbiota and Serotonin and its Impact on Gut Motility. *Curr. Pharm. Biotechnol.* **2018**, *19*, 190–195. [[CrossRef](#)]
86. Christiansen, C.B.; Gabe, M.B.N.; Svendsen, B.; Dragsted, L.O.; Rosenkilde, M.M.; Holst, J.J. The impact of short-chain fatty acids on GLP-1 and PYY secretion from the isolated perfused rat colon. *Am. J. Physiol. Gastrointest. Liver Physiol.* **2018**, *315*, G53–G65. [[CrossRef](#)]
87. Psichas, A.; Sleeth, M.L.; Murphy, K.G.; Brooks, L.; Bewick, G.A.; Hanyaloglu, A.C.; Ghatei, M.A.; Bloom, S.R.; Frost, G. The short chain fatty acid propionate stimulates GLP-1 and PYY secretion via free fatty acid receptor 2 in rodents. *Int. J. Obes. (Lond.)* **2015**, *39*, 424–429. [[CrossRef](#)]
88. Ma, Y.; Lee, E.; Yoshikawa, H.; Noda, T.; Miyamoto, J.; Kimura, I.; Hatano, R.; Miki, T. Phloretin suppresses carbohydrate-induced GLP-1 secretion via inhibiting short chain fatty acid release from gut microbiome. *Biochem. Biophys. Res. Commun.* **2022**, *621*, 176–182. [[CrossRef](#)]
89. Canfora, E.E.; Jocken, J.W.; Blaak, E.E. Short-chain fatty acids in control of body weight and insulin sensitivity. *Nat. Rev. Endocrinol.* **2015**, *11*, 577–591. [[CrossRef](#)]
90. Muller, M.; Hernandez, M.A.G.; Goossens, G.H.; Reijnders, D.; Holst, J.J.; Jocken, J.W.E.; van Eijk, H.; Canfora, E.E.; Blaak, E.E. Circulating but not faecal short-chain fatty acids are related to insulin sensitivity, lipolysis and GLP-1 concentrations in humans. *Sci. Rep.* **2019**, *9*, 12515. [[CrossRef](#)]
91. Hernandez, M.A.G.; Canfora, E.E.; Jocken, J.W.E.; Blaak, E.E. The Short-Chain Fatty Acid Acetate in Body Weight Control and Insulin Sensitivity. *Nutrients* **2019**, *11*, 1943. [[CrossRef](#)] [[PubMed](#)]

92. Wexler, H.M. Bacteroides: The good, the bad, and the nitty-gritty. *Clin. Microbiol. Rev.* **2007**, *20*, 593–621. [[CrossRef](#)] [[PubMed](#)]
93. Yang, J.Y.; Lee, Y.S.; Kim, Y.; Lee, S.H.; Ryu, S.; Fukuda, S.; Hase, K.; Yang, C.S.; Lim, H.S.; Kim, M.S.; et al. Gut commensal *Bacteroides acidifaciens* prevents obesity and improves insulin sensitivity in mice. *Mucosal Immunol.* **2017**, *10*, 104–116. [[CrossRef](#)] [[PubMed](#)]
94. Yoshida, N.; Yamashita, T.; Osone, T.; Hosooka, T.; Shinohara, M.; Kitahama, S.; Sasaki, K.; Sasaki, D.; Yoneshiro, T.; Suzuki, T.; et al. *Bacteroides* spp. promotes branched-chain amino acid catabolism in brown fat and inhibits obesity. *iScience* **2021**, *24*, 103342. [[CrossRef](#)] [[PubMed](#)]
95. Mazmanian, S.K.; Kasper, D.L. The love-hate relationship between bacterial polysaccharides and the host immune system. *Nat. Rev. Immunol.* **2006**, *6*, 849–858. [[CrossRef](#)] [[PubMed](#)]
96. Round, J.L.; Mazmanian, S.K. Inducible Foxp3+ regulatory T-cell development by a commensal bacterium of the intestinal microbiota. *Proc. Natl. Acad. Sci. USA* **2010**, *107*, 12204–12209. [[CrossRef](#)] [[PubMed](#)]
97. Ying, W.; Mahata, S.; Bandyopadhyay, G.K.; Zhou, Z.; Wollam, J.; Vu, J.; Mayoral, R.; Chi, N.W.; Webster, N.J.G.; Corti, A.; et al. Catestatin Inhibits Obesity-Induced Macrophage Infiltration and Inflammation in the Liver and Suppresses Hepatic Glucose Production, Leading to Improved Insulin Sensitivity. *Diabetes* **2018**, *67*, 841–848. [[CrossRef](#)] [[PubMed](#)]
98. Ying, W.; Tang, K.; Avolio, E.; Schilling, J.M.; Pasqua, T.; Liu, M.A.; Cheng, H.; Gao, H.; Zhang, J.; Mahata, S.; et al. Immunosuppression of Macrophages Underlies the Cardioprotective Effects of CST (Catestatin). *Hypertension* **2021**, *77*, 1670–1682. [[CrossRef](#)]
99. Muntjewerff, E.M.; Tang, K.; Lutter, L.; Christoffersson, G.; Nicolaisen, M.J.T.; Gao, H.; Katkar, G.D.; Das, S.; Ter Beest, M.; Ying, W.; et al. Chromogranin A regulates gut permeability via the antagonistic actions of its proteolytic peptides. *Acta Physiol. (Oxf.)* **2021**, *232*, e13655. [[CrossRef](#)]
100. Gonzalez-Davila, P.; Schwalbe, M.; Danewalia, A.; Dalile, B.; Verbeke, K.; Mahata, S.K.; El Aidy, S. Catestatin selects for colonization of antimicrobial-resistant gut bacterial communities. *ISME J.* **2022**, *16*, 1873–1882. [[CrossRef](#)]
101. Corb Aron, R.A.; Abid, A.; Vesa, C.M.; Nechifor, A.C.; Behl, T.; Ghitea, T.C.; Munteanu, M.A.; Fratila, O.; Andronie-Cioara, F.L.; Toma, M.M.; et al. Recognizing the Benefits of Pre-/Probiotics in Metabolic Syndrome and Type 2 Diabetes Mellitus Considering the Influence of *Akkermansia muciniphila* as a Key Gut Bacterium. *Microorganisms* **2021**, *9*, 618. [[CrossRef](#)] [[PubMed](#)]
102. Bhutiani, N.; Schucht, J.E.; Miller, K.R.; McClave, S.A. Technical Aspects of Fecal Microbial Transplantation (FMT). *Curr. Gastroenterol. Rep.* **2018**, *20*, 30. [[CrossRef](#)] [[PubMed](#)]
103. Mattila, E.; Uusitalo-Seppala, R.; Wuorela, M.; Lehtola, L.; Nurmi, H.; Ristikankare, M.; Moilanen, V.; Salminen, K.; Seppala, M.; Mattila, P.S.; et al. Fecal transplantation, through colonoscopy, is effective therapy for recurrent *Clostridium difficile* infection. *Gastroenterology* **2012**, *142*, 490–496. [[CrossRef](#)] [[PubMed](#)]
104. Friedman-Korn, T.; Livovsky, D.M.; Maharshak, N.; Aviv Cohen, N.; Paz, K.; Bar-Gil Shitrit, A.; Goldin, E.; Koslowsky, B. Fecal Transplantation for Treatment of *Clostridium Difficile* Infection in Elderly and Debilitated Patients. *Dig. Dis. Sci.* **2018**, *63*, 198–203. [[CrossRef](#)]
105. Cohen, N.A.; Maharshak, N. Novel Indications for Fecal Microbial Transplantation: Update and Review of the Literature. *Dig. Dis. Sci.* **2017**, *62*, 1131–1145. [[CrossRef](#)]
106. Winslet, M.C.; Andrews, H.; Allan, R.N.; Keighley, M.R. Fecal diversion in the management of Crohn’s disease of the colon. *Dis. Colon Rectum* **1993**, *36*, 757–762. [[CrossRef](#)]
107. Grehan, M.J.; Borody, T.J.; Leis, S.M.; Campbell, J.; Mitchell, H.; Wettstein, A. Durable alteration of the colonic microbiota by the administration of donor fecal flora. *J. Clin. Gastroenterol.* **2010**, *44*, 551–561. [[CrossRef](#)]
108. Bakken, J.S.; Borody, T.; Brandt, L.J.; Brill, J.V.; Demarco, D.C.; Franzos, M.A.; Kelly, C.; Khoruts, A.; Louie, T.; Martinelli, L.P.; et al. Treating *Clostridium difficile* infection with fecal microbiota transplantation. *Clin. Gastroenterol. Hepatol.* **2011**, *9*, 1044–1049. [[CrossRef](#)]
109. Gonzalez-Davila, P.; Schwalbe, M.; Danewalia, A.; Wardenaar, R.; Dalile, B.; Verbeke, K.; Mahata, S.K.; El Aidy, S. Gut microbiota transplantation drives the adoptive transfer of colonic genotype-phenotype characteristics between mice lacking catestatin and their wild type counterparts. *Gut Microbes* **2022**, *14*, 2081476. [[CrossRef](#)]
110. Schneeberger, M.; Everard, A.; Gomez-Valades, A.G.; Matamoros, S.; Ramirez, S.; Delzenne, N.M.; Gomis, R.; Claret, M.; Cani, P.D. *Akkermansia muciniphila* inversely correlates with the onset of inflammation, altered adipose tissue metabolism and metabolic disorders during obesity in mice. *Sci. Rep.* **2015**, *5*, 16643. [[CrossRef](#)]
111. Zhou, Q.; Pang, G.; Zhang, Z.; Yuan, H.; Chen, C.; Zhang, N.; Yang, Z.; Sun, L. Association Between Gut *Akkermansia* and Metabolic Syndrome is Dose-Dependent and Affected by Microbial Interactions: A Cross-Sectional Study. *Diabetes Metab. Syndr. Obes.* **2021**, *14*, 2177–2188. [[CrossRef](#)] [[PubMed](#)]
112. Earley, H.; Lennon, G.; Balfe, A.; Coffey, J.C.; Winter, D.C.; O’Connell, P.R. The abundance of *Akkermansia muciniphila* and its relationship with sulphated colonic mucins in health and ulcerative colitis. *Sci. Rep.* **2019**, *9*, 15683. [[CrossRef](#)]
113. Glassner, K.L.; Abraham, B.P.; Quigley, E.M.M. The microbiome and inflammatory bowel disease. *J. Allergy Clin. Immunol.* **2020**, *145*, 16–27. [[CrossRef](#)] [[PubMed](#)]
114. den Besten, G.; van Eunen, K.; Groen, A.K.; Venema, K.; Reijngoud, D.J.; Bakker, B.M. The role of short-chain fatty acids in the interplay between diet, gut microbiota, and host energy metabolism. *J. Lipid Res.* **2013**, *54*, 2325–2340. [[CrossRef](#)]
115. Bolognini, D.; Tobin, A.B.; Milligan, G.; Moss, C.E. The Pharmacology and Function of Receptors for Short-Chain Fatty Acids. *Mol. Pharmacol.* **2016**, *89*, 388–398. [[CrossRef](#)] [[PubMed](#)]

116. Morrison, D.J.; Preston, T. Formation of short chain fatty acids by the gut microbiota and their impact on human metabolism. *Gut Microbes* **2016**, *7*, 189–200. [[CrossRef](#)]
117. De Preter, V.; Geboes, K.P.; Bulteel, V.; Vandermeulen, G.; Suenart, P.; Rutgeerts, P.; Verbeke, K. Kinetics of butyrate metabolism in the normal colon and in ulcerative colitis: The effects of substrate concentration and carnitine on the beta-oxidation pathway. *Aliment. Pharmacol. Ther.* **2011**, *34*, 526–532. [[CrossRef](#)]
118. Huda-Faujan, N.; Abdulmir, A.S.; Fatimah, A.B.; Anas, O.M.; Shuhaimi, M.; Yazid, A.M.; Loong, Y.Y. The impact of the level of the intestinal short chain Fatty acids in inflammatory bowel disease patients versus healthy subjects. *Open Biochem. J.* **2010**, *4*, 53–58. [[CrossRef](#)]
119. Wang, H.B.; Wang, P.Y.; Wang, X.; Wan, Y.L.; Liu, Y.C. Butyrate enhances intestinal epithelial barrier function via up-regulation of tight junction protein Claudin-1 transcription. *Dig. Dis. Sci.* **2012**, *57*, 3126–3135. [[CrossRef](#)]
120. Arpaia, N.; Campbell, C.; Fan, X.; Dikiy, S.; van der Veeken, J.; deRoos, P.; Liu, H.; Cross, J.R.; Pfeffer, K.; Coffey, P.J.; et al. Metabolites produced by commensal bacteria promote peripheral regulatory T-cell generation. *Nature* **2013**, *504*, 451–455. [[CrossRef](#)]
121. Furusawa, Y.; Obata, Y.; Fukuda, S.; Endo, T.A.; Nakato, G.; Takahashi, D.; Nakanishi, Y.; Uetake, C.; Kato, K.; Kato, T.; et al. Commensal microbe-derived butyrate induces the differentiation of colonic regulatory T cells. *Nature* **2013**, *504*, 446–450. [[CrossRef](#)] [[PubMed](#)]
122. Chen, L.; Sun, M.; Wu, W.; Yang, W.; Huang, X.; Xiao, Y.; Ma, C.; Xu, L.; Yao, S.; Liu, Z.; et al. Microbiota Metabolite Butyrate Differentially Regulates Th1 and Th17 Cells' Differentiation and Function in Induction of Colitis. *Inflamm. Bowel. Dis.* **2019**, *25*, 1450–1461. [[CrossRef](#)] [[PubMed](#)]
123. Fregeau, C.J.; Helgason, C.D.; Bleackley, R.C. Two cytotoxic cell proteinase genes are differentially sensitive to sodium butyrate. *Nucleic Acids Res.* **1992**, *20*, 3113–3119. [[CrossRef](#)]
124. Tsuda, H.; Ochiai, K.; Suzuki, N.; Otsuka, K. Butyrate, a bacterial metabolite, induces apoptosis and autophagic cell death in gingival epithelial cells. *J. Periodontal Res.* **2010**, *45*, 626–634. [[CrossRef](#)] [[PubMed](#)]
125. Kennedy, B.P.; Mahata, S.K.; O'Connor, D.T.; Ziegler, M.G. Mechanism of cardiovascular actions of the Chromogranin A fragment catestatin in vivo. *Peptides* **1998**, *19*, 1241–1248. [[CrossRef](#)]
126. Kruger, P.G.; Mahata, S.K.; Helle, K.B. Catestatin (CgA344–364) stimulates rat mast cell release of histamine in a manner comparable to mastoparan and other cationic charged neuropeptides. *Regul. Pept.* **2003**, *114*, 29–35. [[CrossRef](#)]
127. Kojima, M.; Ozawa, N.; Mori, Y.; Takahashi, Y.; Watanabe-Kominato, K.; Shirai, R.; Watanabe, R.; Sato, K.; Matsuyama, T.A.; Ishibashi-Ueda, H.; et al. Catestatin Prevents Macrophage-Driven Atherosclerosis but Not Arterial Injury-Induced Neointimal Hyperplasia. *Thromb. Haemost.* **2018**, *118*, 182–194. [[CrossRef](#)] [[PubMed](#)]
128. Aung, G.; Niyonsaba, F.; Ushio, H.; Kajiwara, N.; Saito, H.; Ikeda, S.; Ogawa, H.; Okumura, K. Catestatin, a neuroendocrine antimicrobial peptide, induces human mast cell migration, degranulation and production of cytokines and chemokines. *Immunology* **2011**, *132*, 527–539. [[CrossRef](#)]
129. Kljakovic-Gaspic, T.; Tokic, D.; Martinovic, D.; Kumric, M.; Supe-Domic, D.; Stojanovic Stipic, S.; Delic, N.; Vrdoljak, J.; Vilovic, M.; Ticinovic Kurir, T.; et al. Prognostic Value of Catestatin in Severe COVID-19: An ICU-Based Study. *J. Clin. Med.* **2022**, *11*, 4496. [[CrossRef](#)]
130. Jati, S.; Kundu, S.; Chakraborty, A.; Mahata, S.K.; Nizet, V.; Sen, M. Wnt5A Signaling Promotes Defense Against Bacterial Pathogens by Activating a Host Autophagy Circuit. *Front. Immunol.* **2018**, *9*, 679. [[CrossRef](#)]
131. Zhang, W.; Carravetta, V.; Plekan, O.; Feyrer, V.; Richter, R.; Coreno, M.; Prince, K.C. Electronic structure of aromatic amino acids studied by soft X-ray spectroscopy. *J. Chem. Phys.* **2009**, *131*, 035103. [[CrossRef](#)] [[PubMed](#)]
132. Matta, C.F.; Hernandez-Trujillo, J.; Tang, T.H.; Bader, R.F. Hydrogen-hydrogen bonding: A stabilizing interaction in molecules and crystals. *Chemistry (Easton)* **2003**, *9*, 1940–1951. [[CrossRef](#)] [[PubMed](#)]
133. Scheiner, S.; Kar, T.; Pattanayak, J. Comparison of various types of hydrogen bonds involving aromatic amino acids. *J. Am. Chem. Soc.* **2002**, *124*, 13257–13264. [[CrossRef](#)] [[PubMed](#)]
134. Dougherty, D.A. Cation-pi interactions involving aromatic amino acids. *J. Nutr.* **2007**, *137*, 1504S–1508S. [[CrossRef](#)] [[PubMed](#)]
135. Dougherty, D.A. The cation-pi interaction. *Acc. Chem. Res.* **2013**, *46*, 885–893. [[CrossRef](#)] [[PubMed](#)]
136. Chelli, R.; Gervasio, F.L.; Procacci, P.; Schettino, V. Stacking and T-shape competition in aromatic-aromatic amino acid interactions. *J. Am. Chem. Soc.* **2002**, *124*, 6133–6143. [[CrossRef](#)]
137. Yajima, T.; Takamido, R.; Shimazaki, Y.; Odani, A.; Nakabayashi, Y.; Yamauchi, O. π - π stacking assisted binding of aromatic amino acids by copper(II)-aromatic diimine complexes. Effects of ring substituents on ternary complex stability. *Dalton Trans.* **2007**, *3*, 299–307. [[CrossRef](#)]
138. Kelkar, D.A.; Chattopadhyay, A. Membrane interfacial localization of aromatic amino acids and membrane protein function. *J. Biosci.* **2006**, *31*, 297–302. [[CrossRef](#)]
139. Brocchieri, L.; Karlin, S. Geometry of interplanar residue contacts in protein structures. *Proc. Natl. Acad. Sci. USA* **1994**, *91*, 9297–9301. [[CrossRef](#)]
140. Meyer, E.A.; Castellano, R.K.; Diederich, F. Interactions with aromatic rings in chemical and biological recognition. *Angew. Chem. Int. Ed. Engl.* **2003**, *42*, 1210–1250. [[CrossRef](#)]
141. Espinoza-Fonseca, L.M. Aromatic residues link binding and function of intrinsically disordered proteins. *Mol. Biosyst.* **2012**, *8*, 237–246. [[CrossRef](#)] [[PubMed](#)]

142. Loladze, V.V.; Ermolenko, D.N.; Makhatadze, G.I. Thermodynamic consequences of burial of polar and non-polar amino acid residues in the protein interior. *J. Mol. Biol.* **2002**, *320*, 343–357. [[CrossRef](#)] [[PubMed](#)]
143. Kellis, J.T., Jr.; Nyberg, K.; Sali, D.; Fersht, A.R. Contribution of hydrophobic interactions to protein stability. *Nature* **1988**, *333*, 784–786. [[CrossRef](#)] [[PubMed](#)]
144. Zhao, N.; Pang, B.; Shyu, C.R.; Korkein, D. Charged residues at protein interaction interfaces: Unexpected conservation and orchestrated divergence. *Protein Sci.* **2011**, *20*, 1275–1284. [[CrossRef](#)]
145. Sahu, B.S.; Obbineni, J.M.; Sahu, G.; Allu, P.K.; Subramanian, L.; Sonawane, P.J.; Singh, P.K.; Sasi, B.K.; Senapati, S.; Maji, S.K.; et al. Functional genetic variants of the catecholamine-release-inhibitory peptide catestatin in an Indian population: Allele-specific effects on metabolic traits. *J. Biol. Chem.* **2012**, *287*, 43840–43852. [[CrossRef](#)]
146. Choi, Y.; Miura, M.; Nakata, Y.; Sugawara, T.; Nissato, S.; Otsuki, T.; Sugawara, J.; Iemitsu, M.; Kawakami, Y.; Shimano, H.; et al. A common genetic variant of the Chromogranin A-derived peptide catestatin is associated with atherosclerosis and hypertension in a Japanese population. *Endocr. J.* **2015**, *62*, 797–804. [[CrossRef](#)]
147. Dhindsa, R.S.; Copeland, B.R.; Mustoe, A.M.; Goldstein, D.B. Natural Selection Shapes Codon Usage in the Human Genome. *Am. J. Hum. Genet.* **2020**, *107*, 83–95. [[CrossRef](#)]
148. McGarrah, R.W.; White, P.J. Branched-chain amino acids in cardiovascular disease. *Nat. Rev. Cardiol.* **2023**, *20*, 77–89. [[CrossRef](#)]
149. Rees, J.S.; Castellano, S.; Andres, A.M. The Genomics of Human Local Adaptation. *Trends Genet.* **2020**, *36*, 415–428. [[CrossRef](#)]
150. Brunner, J.S.; Finley, L.W.S. Metabolic determinants of tumour initiation. *Nat. Rev. Endocrinol.* **2023**, *19*, 134–150. [[CrossRef](#)]
151. Muntjewerff, E.M.; Christoffersson, G.; Mahata, S.K.; van den Bogaart, G. Putative regulation of macrophage-mediated inflammation by catestatin. *Trends Immunol.* **2022**, *43*, 41–50. [[CrossRef](#)] [[PubMed](#)]
152. Zhang, D.; Shooshtarizadeh, P.; Laventie, B.J.; Colin, D.A.; Chich, J.F.; Vidic, J.; de Barry, J.; Chasserot-Golaz, S.; Delalande, F.; Van Dorsselaer, A.; et al. Two Chromogranin A-derived peptides induce calcium entry in human neutrophils by calmodulin-regulated calcium independent phospholipase A2. *PLoS ONE* **2009**, *4*, e4501. [[CrossRef](#)] [[PubMed](#)]

Disclaimer/Publisher’s Note: The statements, opinions and data contained in all publications are solely those of the individual author(s) and contributor(s) and not of MDPI and/or the editor(s). MDPI and/or the editor(s) disclaim responsibility for any injury to people or property resulting from any ideas, methods, instructions or products referred to in the content.